THE JOURNAL OF PHYSICAL CHEMISTRY Letters

Letter

pubs.acs.org/JPCL

Exploring N-Rich Phases in Li_xN_y Clusters for Hydrogen Storage at Nanoscale

Amrita Bhattacharya[†] and Saswata Bhattacharya*[,‡]

[†]Fritz-Haber-Institut der Max-Planck-Gesellschaft, Faradayweg 4-6, D-14195 Berlin, Germany

[‡]Department of Physics, Indian Institute of Technology Delhi, Hauz Khas, 110016 New Delhi, India

ABSTRACT: We have performed cascade genetic algorithm and ab initio atomistic thermodynamics under the framework of first-principles-based hybrid density functional theory to study the (meta-)stability of a wide range of Li_xN_y clusters. We found that hybrid xc-functional is essential to address this problem as a local/semilocal functional simply fails even to predict a qualitative prediction. Most importantly, we find that though in bulk lithium nitride, the Li-rich phase, that is, Li_3N, is the stable stoichiometry; in small Li_xN_y clusters, N-rich phases are more stable at thermodynamic equilibrium. We further show that these N-rich clusters are promising hydrogen storage material because of their easy adsorption and desorption ability at respectively low (≤300 K) and moderately high temperature (≥600 K).

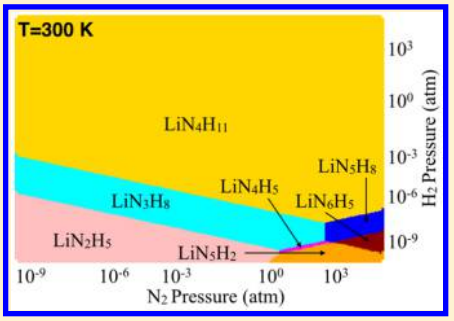

Hydrogen is the most abundant element in the universe that contains the highest energy density per unit mass, and when it burns, it produces only water and energy. In view of this, it has been considered to be one of the promising solutions for the clean alternative energies.[1−3] Significant amount of research initiatives have been taken place along this direction,[4−7] but unfortunately, hydrogen is needed to be produced from water or other solid-state materials as it is not freely available in nature. Therefore, although hydrogen can be considered as renewable, if it is produced from water, it costs more energy to get produced than the energy one recovers on burning it. This necessitates designing of promising solid-state materials or nanostructures, where hydrogen molecules can be stored. This has been, therefore, an active field of research for the last few decades and various kinds of materials such as metal hydrides,[4,8,9] clusters,[10−17] nanostructures,[18−24] highly porous metal−organic frameworks (MOFs),[5,6,25−28] clathrate hydrates,[29−31] covalent organic frameworks (COFs),[32,33] and so forth have been studied extensively. In particular, complex binary hydrides involving light metals such as Li, Mg, Ca, and so forth have been extensively investigated because of their high gravimetric storage capacity. Among them, lithium nitride [Li_3N], lithium imide [Li_2NH], or amide [$LiNH_2$] have been found to exhibit strong affinity for H_2 because of the reversible reactions $Li_3N + 2H_2 \leftrightarrow Li_2NH + LiH + H_2 \leftrightarrow LiNH_2 + 2LiH$.[34] Unfortunately, though this material can store sufficiently high amount of hydrogen, the desorption kinetics is poor for its on-board practical application. Li atoms being ionized as Li^+ cations, strongly attracts $[NH_2]^-$ complex anion and thereby form a strong bond, which is rather difficult to break at moderate temperature.[7] In order to lower the desorption temperature to a permissible range, doping with suitable metal adatoms have already been tried.[7,35]

We have explored the possibility of realizing clusters of these materials. It has been found that reducing the number of particles in a cluster reveals the possibility of several interesting properties. In a range where matter is reduced to sizes of only a few atoms, the intrinsic properties of the so-called clusters are nonscalable from their bulk analogues. We expect that significant amount of hydrogen adsorption would be possible in a nondissociative manner due to presence of high surface-to-bulk ratio and due to the weak dispersive interactions the hydrogen desorption could be favorable. In past, it is been studied to understand the hydrogen storage efficiency of small lithium amide clusters $[LiNH_2]_n$ using ab initio molecular orbital theory.[36] But materials' properties change under operational environment (e.g., temperature (T) and pressure (p) in an atmosphere of reactive molecules). The thermodynamics and kinetics at the relevant temperature (T) and the nature of the environment determine the composition and structure of clusters. In thermodynamic equilibrium, only structures and compositions that minimize the Gibbs' free energy of formation of the composite cluster + ligands(gas) system will be the most stable. Therefore, one has to first ensure the most stable phases and compositions of such clusters at thermodynamic equilibrium. And after that, the efficiency of hydrogen storage should be aimed at. To date, no such consistent theoretical study has been performed, in the field of hydrogen storage in small clusters, that has considered the (meta-)stability of the clusters by including the effect of temperature and pressure of the reactive environment. In this Letter, we address the issue of stability and metastability using our model system that has significance in many practical applications. Our model includes free metal (Li) clusters in (a) a nitrogen-only atmosphere and then in (b) an atmosphere of

Received: July 7, 2015
Accepted: August 31, 2015
Published: August 31, 2015

DOI: 10.1021/acs.jpclett.5b01435
J. Phys. Chem. Lett. 2015, 6, 3726−3730

both nitrogen and hydrogen. It should be noted that we have addressed the situation under thermodynamic equilibrium, whereas the real system might not be always in thermodynamic equilibrium. However, we emphasize that a thermodynamic phase diagram acts as guideline and depicts its limit for predicting properties and functions of real materials.

We have considered first a wide range of Li_xN_y clusters, where x = 1, 2, ..., 6, 9, 12, 15, 18 and y is determined by thermal equilibrium with the environment at given temperature T and partial nitrogen pressure p_{N_2} [We varied the y value starting from 1, 2, 3, ... and kept on increasing it until when the specific Li_xN_y stoichiometry goes totally outside our phase diagrams, that is, under no circumstances that stoichiometry can be important in the environmental conditions, which we have considered here.] To get the minimum energy configurations, for each stoichiometry, the total energy is minimized with respect to both geometry and spin state. Very unexpectedly, our results reveal that though in bulk Li_3N is the most stable phase, in small clusters, the stoichiometry of the most stable phase is quite different.

The low energy structures (including the global minimum (GM)) are generated from an exhaustive scanning of the potential energy surface (PES) from our recent implementation of cascade genetic algorithm. The term cascade means a multistepped algorithm where successive steps employ higher level of theory and each of the next level takes information obtained at its immediate lower level. Typically, the cascade GA starts from a crude but sophisticated classical force field and goes up to density functional theory using hybrid functionals. This GA algorithm's implementation is thoroughly benchmarked and validated (with respect to more advanced theory) in details in refs 37 and 38.

We have performed the density functional theory (DFT) calculations using FHI-aims, which is an all electron code with numerical atom centered basis sets.[39] The low energy GA structures are further optimized at a higher level settings, where energy minimization is performed with vdW-corrected-PBE +vdW[40] functional, "tight tier 2" settings, and force tolerance was set to better than 10^{-5} eV/Å. The van der Waals correction is calculated as implemented in Tkatchenko−Scheffler scheme.[41] Finally the total single point energy is calculated afterward on top of this optimized structure via vdW-corrected PBE0[42] hybrid xc functional (PBE0+vdW), with "tight tier 2" settings. [As described in detail in ref 38, in our cascade GA, the latter energy is used to evaluate the fitness function, i.e., a mapping of the energy interval between highest- and lowest-energy cluster in the running pool into the interval [0, 1]. Obviously, the higher the value of the fitness function for a cluster, the higher is the probability of selecting it for generating a new structure.] We find that PBE+vdW energetics strongly overestimates stability of clusters with larger y values in Li_xN_y clusters. This results a qualitatively wrong prediction that adsorption of N_2 could be favored over desorption up to a large excess of nitrogen. Such behavior is not confirmed by hybrid functional [e.g HSE06+vdW,[43] PBE0+vdW] as employed in our calculations. The difference in energetics of PBE0+vdW and HSE06+vdW is always within 0.05 eV. The spin states of the clusters are also different as found by PBE+vdW and PBE0+vdW/HSE06+vdW. In view of this, all our results are thoroughly tested and benchmarked w.r.t hybrid functionals (PBE0+vdW) using "tight" numerical settings and tier 2 basis set.[39] [Note that while plotting phase diagram, we actually consider the difference in free energy where about 80% contribution comes from electronic total energy. Now if the electronic total energy is at the order of 0.03 eV error bar, the differences of such contributions surely won't make any significant change in the phase diagram as shown in the figures in our manuscript. Thus, we are sure that PBE0+vdW energetics at PBE+vdW geometry makes perfect sense, especially to avoid long computational cost in optimizing the structure at the PBE0+vdW level without any gain/change in the outcome/conclusion of the paper. Moreover, we have also verified that the Li−N equilibrium bond distance is correctly predicted (within an error bar of 2%) by PBE+vdW with respect to renormalized perturbation theory with second order screened exchange (rPT2).[44]]

The free energy of the low energy isomers [We have considered all the isomers within an energy window of 0.5 eV from the global minimum (GM) as we have seen that it is very unlikely that isomers above 0.5 eV from the GM would become more stable after including their translational, rotational, vibrational, spin and symmetry free energy contributions to the total energy.] (in the PES) is then calculated as a function of T and p_{N_2} for each stoichiometry using the ab initio atomistic thermodynamics (aiAT) approach. The concept of aiAT is earlier developed and successfully applied initially for bulk semiconductors[45] and later applied to the study of oxide formation at the surface of some transition metals and other materials.[46] We have recently extended this approach to cluster systems[37] following our detailed description as in ref 38. Therefore, from different cluster compositions and structures with the lowest free energy the thermodynamic phase diagram can be constructed as a function of T and p_{N_2}. One such phase diagram is shown in Figure 1. At a given T, p_{N_2}, and y, the stable

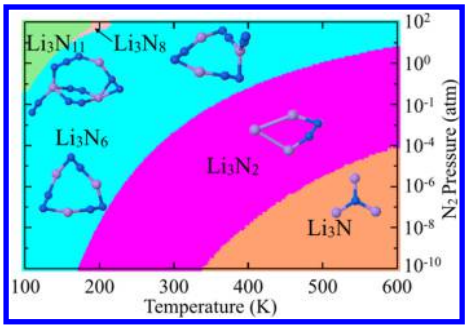

Figure 1. Phase diagram for Li_3N_x clusters in an nitrogen atmosphere. The geometries are optimized with PBE+vdW and the total energies are calculated with PBE0+vdW.

stoichiometry of a Li_xN_y cluster is determined via aiAT, that is, by minimizing the Gibbs' free energy of formation $\Delta G_f(T, p_{N_2})$

$$\Delta G_f(T, p_{N_2}) = F_{Li_xN_y}(T) - F_{Li_x}(T) - y \times \mu_N(T, p_{N_2}) \quad (1)$$

Here, $F_{Li_xN_y}(T)$ and $F_{Li_x}(T)$ are the Helmholtz free energies of the Li_xN_y and the pristine Li_x cluster [The clusters are at their ground state configuration with respect to geometry and spin, respectively.] and $\mu_N(T,p_{N2})$ is the chemical potential of nitrogen. As explained in ref 38, $F_{Li_xN_y}(T)$ and $F_{Li_x}(T)$ are calculated using DFT information and are calculated from the sum of DFT total energy, DFT vibrational free energy in the harmonic approximation, as well as translational, rotational,

DOI: 10.1021/acs.jpclett.5b01435
J. Phys. Chem. Lett. 2015, 6, 3726−3730

symmetry, and spin-degeneracy free-energy contributions. The dependence of $\mu_N(T, p_{N_2})$ on T and p_{N_2} is calculated using the ideal (diatomic) gas approximation with the same DFT functional as for the clusters. The phase diagram for a particular Li_xN_y is constructed by identifying the lowest free-energy structures at each T, p_{N_2}. As a representative example, we show in Figure 1 the phase diagram for $x = 3$. Note that surprisingly in small cluster, we find that at a realistic T and p_{N_2}, N-rich phases are becoming more stable over the conventionally known most stable phase Li_3N as in bulk. We have then extended our observation for a wide range of clusters of Li_xN_y configuration varying x as 1, 2, ..., 6, 9, 12, 15, 18 and y is increased as 1, 2, 3, ... as per the highest possible value at each x in the thermodynamic condition as employed in the phase diagrams. For example, for $x = 3$, we see from Figure 1 the highest possible y is 11. We find that the N-rich phase in these small clusters are consistently becoming quite stable over a wide range of (T, p_{N_2}) environmental conditions. This is shown in Figure 2, where we have plotted the most stable

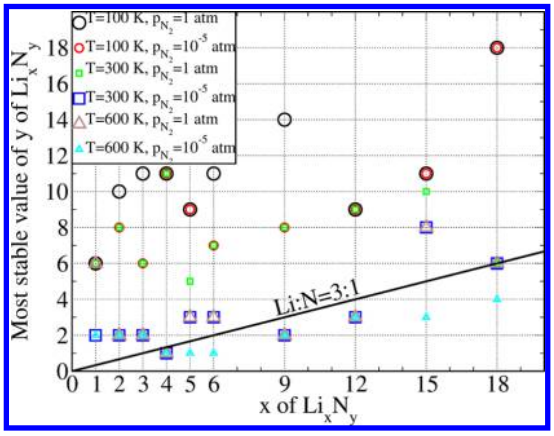

Figure 2. (color online) The most stable Li_xN_y clusters at various temperatures and pressures under thermodynamic equilibrium. The geometries are optimized with PBE+vdW, and the electronic energy is calculated using PBE0+vdW.

stoichiometry of y at different (T, p_{N_2}) with varying x values. The black line represents the usual Li:N = 3:1 stoichiometry as in bulk. Note that most of the stable phases are above this black line and are significantly high N-rich especially for small clusters. As expected, due to quantum size effect, the reactivity of the larger clusters get decreased with growing size. But still even at larger sizes, the clusters are more N-rich as compared to their bulk limit. Only at high temperature (>600 K) and low pressure ($<10^{-5}$ atm) the clusters are N-deficient.

Subsequently, we explored the efficiency of the N-rich phases of these cluster as hydrogen storage material. However, the procedure for this is not easy as one has to understand under which temperature conditions and in which N_2 and H_2 (partial) pressure range these nanoclusters become more stable, that is, under which optimum conditions the N_2 and H_2 adsorption can take place on the surface of a given cluster size. Note that under reaction conditions, the nanocluster comprises of a wide range of structures including different number of atoms with various oxidation states, all of which could be active to some extent in the reaction. Some obvious questions arise naturally, for example, "which are the species present in the real reaction and what are their structures?" It is also interesting to understand "how the nanocluster changes their structure and properties upon adsorption of a different ligand molecules? We have addressed these questions on considering another ligand (e.g., H_2) adsorbed onto LiN_y clusters forming LiN_yH_z clusters and tried to understand the stability of the entire system in the presence of both N_2 + H_2 pressures. In order to fulfil these aims, small clusters LiN_yH_z are first thoroughly scanned from our cascade genetic algorithm implementation and their stability is studied using atomistic thermodynamics to mimic an atmosphere composed of N_2 and H_2 gases at realistic temperature and pressure conditions. As depicted in eq 1, here to address the (meta-)stability of LiN_yH_z clusters, in the presence of one more additional ligand, that is, H_2, the equation gets modified as below

$$\Delta G_f(T, p_{N_2}, p_{H_2}) = F_{LiN_yH_z}(T) - F_{Li}(T) - y \times \mu_N(T, p_{N_2}) - z \times \mu_H(T, p_{H_2}) \quad (2)$$

Here, $F_{LiN_yH_z}(T)$ and $F_{Li}(T)$ are the Helmholtz free energies of the LiN_yH_z and the pristine Li cluster (in this case single Li atom), respectively. Like as before in eq 1, here also we have calculated this from the sum of PBE0 DFT total energy, DFT vibrational free energy (in the harmonic approximation), and translational, rotational, symmetry, spin-degeneracy free-energy contributions. $\mu_N(T,p_{N_2})$ and $\mu_H(T,p_{H_2})$ are the chemical potential of nitrogen and hydrogen, respectively.

In Figure 3, we have compared the phase diagrams of the stability of LiN_yH_z clusters, varying H_2 and N_2 pressures, at two

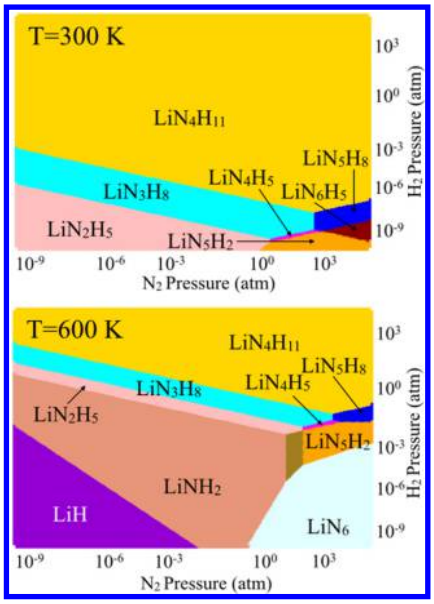

Figure 3. (color online) Phase diagram of LiN_yH_z at varying pressure of p_{H_2} and p_{N_2} of two different temperatures T = 300 K (top) and T = 600 K (bottom).

different temperatures (viz. 300 K (top) and 600 K (bottom)). It is clear from Figure 3 that at T = 300 K, the small clusters can adsorb quite a substantial amount of hydrogen at a realistic temperature and pressure. Note that in bulk Li_3N, the highest amount of hydrogen uptake is possible when it forms lithium amides/imides ($LiNH_2$/Li_2NH). But in small clusters, the situation is very different as LiN_4H_{11} is thermodynamically the most stable cluster and the material is stable over a wide

DOI: 10.1021/acs.jpclett.5b01435
J. Phys. Chem. Lett. 2015, 6, 3726−3730

experimentally achievable region in the phase diagram at T = 300 K.

It should be noted that for an efficient hydrogen storage materials, the desorption kinetics should also need to be optimal. We have provided a similar phases diagram in the bottom panel of Figure 3 at T = 600 K. We find that at this temperature first the stability region of LiN_4H_{11} is reduced, and less H-rich phases (viz. LiN_3H_8, LiN_2H_5, $LiNH_2$) become more stable. This means the cluster tends to release hydrogen at higher temperature, whereas the H-rich phase being absolutely stable at room temperature. On a critical look at the phase diagram, it appears to be that under a fixed pressure region of both p_{H_2} and p_{N_2}, if we simply increase temperature, these type of clusters have a tendency to release ammonia (NH_3) molecule. This is shown more clearly in Figure 4. It is evident

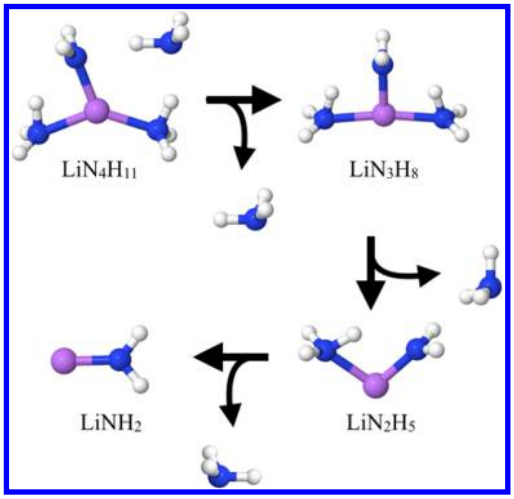

Figure 4. (color online) Release of three units of ammonia from LiN_4H_{11} before the final product $LiNH_2$ is formed at a varying T, p_{N_2}, p_{H_2}.

from Figure 3 that on increasing temperature these nanoclusters will form a reversible cycle under a constant p_{H_2} and p_{N_2}, where the following reaction is going on as shown in Figure 4

$$\begin{aligned} LiN_4H_{11} &\rightarrow LiN_3H_8 + NH_3 \\ &\rightarrow LiN_2H_5 + NH_3 \\ &\rightarrow LiNH_2 + NH_3 \end{aligned} \quad (3)$$

It should be mentioned that commenting on the reaction kinetics is rather difficult and beyond the level of theory we employed here. This needs much in-depth study to understand the reaction kinetics. However, if we assume the reaction kinetics to be what we see from the individual $Li_1N_xH_z$ phase diagram, the reaction activation barrier from one stoichiometry to other should be within a reasonable range. Therefore, we have performed nudged elastic band (NEB) calculations and found that the reaction activation barrier is never more than 20−30 kJ/mol for the above reaction as stated in eq 3. Thus, we see that just by changing temperature, we can get three units of NH_3 out of this LiN_4H_{11}. Therefore, using a robust methodology first, we introduced a new class of N-rich clusters for storing a large amount of hydrogen and finally if this reaction is to be true to get such an automatic release of ammonia, it solves the problem of hydrogen storage, as hydrogen can be released economically from ammonia on-demand, without the need for high-pressure or cryogenic storage.[47]

In summary, we have employed our massively parallel cascade genetic algorithm to scan the potential energy surface of a large number of Li_xN_y clusters. We find that a local/semilocal functional is not correct even to find a reasonably qualitative prediction. In view of this, we have employed more advanced hybrid DFT functional PBE0 to calculate accurately the energetics throughout our calculations. We find by applying aiAT, that the behavior of small Li_xN_y clusters are very different than their bulk, which may be due to quantum confinement effect. In small clusters, over a wide range of sizes, N-rich phases are consistently stable at thermodynamic equilibrium under experimentally achievable temperature and pressure p_{N_2}. We, therefore, presumably for the first time, introduce a new class of clusters that has been overlooked in the past. We went one step further to understand the effectiveness of these clusters in the field of hydrogen storage. We generated a large number of $Li_xN_yH_z$ clusters out of which one of the test cases is shown here for LiN_yH_z. These clusters can store significantly high amount of hydrogen and thereby should possess wide application as possible hydrogen storage materials.

AUTHOR INFORMATION

Corresponding Author

*E-mail: saswata@physics.iitd.ac.in. Phone: +91-26591359. Fax: +91-26582037.

Notes

The authors declare no competing financial interest.

REFERENCES

(1) Zuttel, A. Materials for hydrogen storage. *Mater. Today* **2003**, *6*, 24−33.
(2) Schlapbach, L.; Zuttel, A. Hydrogen-storage materials for mobile applications. *Nature* **2001**, *414*, 353−358.
(3) Jena, P. Materials for hydrogen storage: past, present, and future. *J. Phys. Chem. Lett.* **2011**, *2*, 206−211.
(4) Orimo, S.; Nakamori, Y.; Eliseo, J.; Zuttel, A. Complex hydrides for hydrogen storage. *Chem. Rev.* **2007**, *107*, 4111−4132.
(5) Suh, M.; Park, H.; Prasad, T.; Lim, D. Hydrogen storage in metal−organic frameworks. *Chem. Rev.* **2012**, *112*, 782−835.
(6) Murray, L.; Dinca, M.; Long, J. Hydrogen storage in metal—organic frameworks. *Chem. Soc. Rev.* **2009**, *38*, 1294−1314.
(7) Bhattacharya, S.; Wu, G.; Ping, C.; Feng, Y. P.; Das, G. P. Lithium Calcium Imide [$Li_2Ca(NH)_2$] for Hydrogen Storage: Structural and Thermodynamic Properties. *J. Phys. Chem. B* **2008**, *112*, 11381−11384. PMID:18710276
(8) Sakintuna, B.; Lamari-Darkrim, F.; Hirscher, M. Metal hydride materials for solid hydrogen storage: a review. *Int. J. Hydrogen Energy* **2007**, *32*, 1121−1140.
(9) Jain, I.; Lal, C.; Jain, A. Hydrogen storage in Mg: a most promising material. *Int. J. Hydrogen Energy* **2010**, *35*, 5133−5144.
(10) Bhattacharya, S.; Xiong, Z.; Wu, G.; Chen, P.; Feng, Y. P.; Majumder, C.; Das, G. P. Dehydrogenation Mechanism of Monoammoniated Lithium Amidoborane [$Li(NH_3)NH_2BH_3$]. *J. Phys. Chem. C* **2012**, *116*, 8859−8864.
(11) Jose, D.; Datta, A. Structures and electronic properties of silicene clusters: a promising material for FET and hydrogen storage. *Phys. Chem. Chem. Phys.* **2011**, *13*, 7304−7311.
(12) Watari, N.; Ohnishi, S.; Ishii, Y. Hydrogen storage in Pd clusters. *J. Phys.: Condens. Matter* **2000**, *12*, 6799.

DOI: 10.1021/acs.jpclett.5b01435
J. Phys. Chem. Lett. 2015, 6, 3726−3730

(13) Wagemans, R.; Lenthe, J. v. Hydrogen storage in magnesium clusters: quantum chemical study. *J. Am. Chem. Soc.* **2005**, *127*, 16675−16680.
(14) Sun, Q.; Wang, Q.; Jena, P.; Kawazoe, Y. Clustering of Ti on a C60 surface and its effect on hydrogen storage. *J. Am. Chem. Soc.* **2005**, *127*, 14582−14583.
(15) Sun, Q.; Jena, P.; Wang, Q.; Marquez, M. First-principles study of hydrogen storage on Li12C60. *J. Am. Chem. Soc.* **2006**, *128*, 9741−9745.
(16) Li, M.; Li, Y.; Zhou, Z.; Shen, P.; Chen, Z. Ca-coated boron fullerenes and nanotubes as superior hydrogen storage materials. *Nano Lett.* **2009**, *9*, 1944−1948.
(17) Koukaras, E.; Zdetsis, A. Ab initio study of Magnesium and Magnesium hydride nanoclusters and nanocrystals: Examining optimal structures and compositions for efficient hydrogen storage. *J. Am. Chem. Soc.* **2012**, *134*, 15914−15922.
(18) Norberg, N.; Arthur, T.; Fredrick, S. Size-dependent hydrogen storage properties of Mg nanocrystals prepared from solution. *J. Am. Chem. Soc.* **2011**, *133*, 10679−10681.
(19) Wang, Q.; Sun, Q.; Jena, P.; Kawazoe, Y. Potential of AlN nanostructures as hydrogen storage materials. *ACS Nano* **2009**, *3*, 621−626.
(20) Arico, A.; Bruce, P.; Scrosati, B.; Tarascon, J. Nanostructured materials for advanced energy conversion and storage devices. *Nat. Mater.* **2005**, *4*, 366−377.
(21) Bhattacharya, S.; Bhattacharya, A.; Das, G. P. Anti-Kubas Type Interaction in Hydrogen Storage on a Li Decorated BHNH Sheet: A First-Principles Based Study. *J. Phys. Chem. C* **2012**, *116*, 3840−3844.
(22) Bhattacharya, S.; Majumder, C.; Das, G. P. Hydrogen Storage in Ti-Decorated BC4N Nanotube. *J. Phys. Chem. C* **2008**, *112*, 17487−17491.
(23) Bhattacharya, S.; Majumder, C.; Das, G. P. Ti-Decorated BC4N Sheet: A planar Nanostructure for High-Capacity Hydrogen Storage. *J. Phys. Chem. C* **2009**, *113*, 15783−15787.
(24) Bhattacharya, A.; Bhattacharya, S.; Majumder, C.; Das, G. P. Transition-Metal Decoration Enhanced Room-Temperature Hydrogen Storage in a Defect-Modulated Graphene Sheet. *J. Phys. Chem. C* **2010**, *114*, 10297−10301.
(25) Rowsell, J.; Yaghi, O. Strategies for hydrogen storage in metal—organic frameworks. *Angew. Chem., Int. Ed.* **2005**, *44*, 4670−4679.
(26) Kesanli, B.; Cui, Y.; Smith, M.; Bittner, E. Highly interpenetrated metal—organic frameworks for hydrogen storage. *Angew. Chem., Int. Ed.* **2005**, *44*, 72−75.
(27) Wong-Foy, A.; Matzger, A. Exceptional H_2 saturation uptake in microporous metal-organic frameworks. *J. Am. Chem. Soc.* **2006**, *128*, 3494−3495.
(28) Li, H.; Eddaoudi, M.; O'Keeffe, M.; Yaghi, O. Design and synthesis of an exceptionally stable and highly porous metal-organic framework. *Nature* **1999**, *402*, 276−279.
(29) Florusse, L.; Peters, C.; Schoonman, J.; Hester, K. Stable low-pressure hydrogen clusters stored in a binary clathrate hydrate. *Science* **2004**, *306*, 469−471.
(30) Lee, H.; Lee, J.; Park, J.; Seo, Y.; Zeng, H.; Moudrakovski, I. Tuning clathrate hydrates for hydrogen storage. *Nature* **2005**, *434*, 743−746.
(31) Chapoy, A.; Anderson, R.; Tohidi, B. Low-pressure molecular hydrogen storage in semi-clathrate hydrates of quaternary ammonium compounds. *J. Am. Chem. Soc.* **2007**, *129*, 746−747.
(32) Han, S.; Furukawa, H.; Yaghi, O. Covalent organic frameworks as exceptional hydrogen storage materials. *J. Am. Chem. Soc.* **2008**, *130*, 11580−11581.
(33) Klontzas, E.; Tylianakis, E. Hydrogen storage in 3D covalent organic frameworks. A multiscale theoretical investigation. *J. Phys. Chem. C* **2008**, *112*, 9095−9098.
(34) Chen, P.; Xiong, Z.; Luo, J.; Lin, J.; Tan, K. Interaction of hydrogen with metal nitrides and imides. *Nature* **2002**, *420*, 302−304.
(35) Moyses Araujo, C.; Scheicher, R. H.; Jena, P.; Ahuja, R. On the structural and energetic properties of the hydrogen absorber $Li_2Mg(NH)_2$. *Appl. Phys. Lett.* **2007**, *91*, 091924−091927.
(36) Li, L.; Peng, B.; Tao, Z.; Cheng, F.; Chen, J. A Quantum-Chemical Study on Understanding the Dehydrogenation Mechanisms of Metal (Na, K, or Mg) Cation Substitution in Lithium Amide Nanoclusters. *Adv. Funct. Mater.* **2010**, *20*, 1894−1902.
(37) Bhattacharya, S.; Levchenko, S. V.; Ghiringhelli, L. M.; Scheffler, M. Stability and Metastability of Clusters in a Reactive Atmosphere: Theoretical Evidence for Unexpected Stoichiometries of MgMOx. *Phys. Rev. Lett.* **2013**, *111*, 135501−135505.
(38) Bhattacharya, S.; Levchenko, S. V.; Ghiringhelli, L. M.; Scheffler, M. Efficient ab initio schemes for finding thermodynamically stable and metastable atomic structures: Benchmark of cascade genetic algorithms. *New J. Phys.* **2014**, *16*, 123016.
(39) Blum, V.; Gehrke, R.; Hanke, F.; Havu, P.; Havu, V.; Ren, X.; Reuter, K.; Scheffler, M. *Comput. Phys. Commun.* **2009**, *180*, 2175.
(40) Perdew, J.; Burke, K.; Ernzerhof, M. Generalized gradient approximation made simple (vol 77, pg 3865, 1996). *Phys. Rev. Lett.* **1997**, *78*, 1396−1396.
(41) Tkatchenko, A.; Scheffler, M. Accurate molecular van der Waals interactions from ground-state electron density and free-atom reference data. *Phys. Rev. Lett.* **2009**, *102*, 073005.
(42) Perdew, J.; Emzerhof, M.; Burke, K. Rationale for mixing exact exchange with density functional approximations. *J. Chem. Phys.* **1996**, *105*, 9982−9985.
(43) Heyd, J.; Scuseria, G. E.; Ernzerhof, M. Erratum:Hybrid functionals based on a screened Coulomb potential[J. Chem. Phys. 118, 8207 (2003)]. *J. Chem. Phys.* **2006**, *124*, 219906−219906.
(44) Ren, X.; Rinke, P.; Joas, C.; Scheffler, M. Random-phase approximation and its applications in computational chemistry and materials science. *J. Mater. Sci.* **2012**, *47*, 7447−7471.
(45) Scheffler, M.; Weinert, C. In *Defects in Semiconductors*; Bardeleben, H. J. v., Ed.; Trans. Tech. Publ. Ltd.: Switzerland, 1986; pp 25−30.
(46) Reuter, K.; Stampf, C.; Scheffler, M. In *Handbook of Materials Modeling*; Yip, S., Ed.; Springer: Netherlands, 2005; pp 149−194.
(47) Lan, R.; Irvine, J.; Tao, S. Ammonia and related chemicals as potential indirect hydrogen storage materials. *Int. J. Hydrogen Energy* **2012**, *37*, 1482−1494.

DOI: 10.1021/acs.jpclett.5b01435
J. Phys. Chem. Lett. 2015, 6, 3726−3730